Insulator–metal phase transition of $Pr_{0.6}Ca_{0.4}MnO_3$ studied by x-ray absorption spectroscopy in pulsed magnetic fields

2009 J. Phys.: Condens. Matter 21 016006

(http://iopscience.iop.org/0953-8984/21/1/016006)

J. Phys.: Condens. Matter **21** (2009) 016006 (5pp) doi:10.1088/0953-8984/21/1/016006

Insulator–metal phase transition of $Pr_{0.6}Ca_{0.4}MnO_3$ studied by x-ray absorption spectroscopy in pulsed magnetic fields

Z W Ouyang[1], Y H Matsuda[1,2], H Nojiri[1], Y Inada[3], Y Niwa[3] and T Arima[4]

[1] Institute for Materials Research, Tohoku University, Sendai 980-8577, Japan
[2] PRESTO, Japan Science and Technology Agency, 4-1-8 Honcho Kawaguchi, Saitama 332-0012, Japan
[3] Photon Factory, Institute of Materials Structure Science, High Energy Accelerator Research Organization, Oho, Tsukuba 305-0801, Japan
[4] Institute of Multidisciplinary Research for Advanced Materials, Tohoku University, Sendai 980-8577, Japan

E-mail: ymatsuda@issp.u-tokyo.ac.jp

Received 22 September 2008, in final form 30 October 2008
Published 2 December 2008
Online at stacks.iop.org/JPhysCM/21/016006

Abstract

Evolution of the Mn K-edge x-ray absorption near edge structure (XANES) in $Pr_{0.6}Ca_{0.4}MnO_3$ at pulsed magnetic fields has been investigated. A small enhancement of XANES spectra is detected across the magnetic-field-induced transition from the charge- and orbital-ordered (COO) insulator to ferromagnetic metal at 20 K. It is found that the magnetic-field dependence of the enhancement shows clear hysteresis, as seen in the magnetization with metamagnetic transition, suggesting a significant correlation between the change in the XANES and the field-induced collapse of the COO state. The enhancement of the absorption can be explained by an increase of the 4p density of states due to a reduction of hybridization between the 4p state of the central Mn ion with the core hole and the neighboring Mn 3d state. Local structural change around Mn ions is expected to modify the strength of the hybridization.

1. Introduction

The doped perovskite manganites $R_{1-x}A_xMnO_3$ (R is a trivalent rare-earth ion and *A* is an alkaline-earth divalent ion) have been intensively investigated due to a wide range of interesting properties, such as colossal magnetoresistance (CMR), charge ordering, orbital ordering, and Jahn–Teller distortion [1–9]. For instance, $La_{1-x}Ca_xMnO_3$, which is one of the most intensively studied manganites, exhibits a paramagnetic (PM) insulator to ferromagnetic (FM) metal transition upon cooling in a broad range of doping ($\sim 0.2 < x < 0.5$) [2]. Such an insulator–metal transition is usually explained within the framework of double exchange-like mechanisms [10] based on the exchange of e_g electrons between Mn^{3+} and Mn^{4+} ions. The electron transfer integral between the Mn ions is increased when the localized t_{2g} spins align ferromagnetically. Thus, the electronic state is significantly correlated with the PM–FM transition [11].

It was, however, also proposed that in addition to the standard double exchange mechanism a strong electron–phonon interaction arising from the Jahn–Teller effect plays a crucial role [12–14]. At the atomic level, the MnO_6 octahedron is distorted significantly in the PM state due to the Jahn–Teller effect of Mn^{3+}, resulting in the splitting of Mn–O distances into four short bonds and two long bonds. This local distortion was intensively studied in $La_{1-x}Ca_xMnO_3$ by x-ray absorption spectroscopy (XAS) [5–7, 15–17]. The XAS shows that the local distortion is correlated with polarons and nearly removed in the FM state [15–17]. Apart from the Mn–O bond distance, the tilting of the MnO_6 octahedron can be correlated with the insulator–metal transition. The transfer of

the e_g electron depends on the Mn^{3+}–Mn^{4+} bond angle through the hybridization between the Mn 3d and O 2p orbitals [18].

Although there have been number of XAS studies of manganites on the transition from the charge-ordered or paramagnetic insulator to ferromagnetic metal state, there is not a wide variety of the materials, i.e. only the $La_{1-x}Ca_xMnO_3$ system has been intensively studied [5–7, 15–17]. Reports on other manganites are found to be limited [3, 19]. It should also be noted that most of the XAS studies have focused on the extended x-ray absorption fine structure (EXAFS) region. The absorption near edge region, where the density of state of the final state of the absorption is directly reflected [20, 21], has only been investigated in detail in a few reports [3, 4]. The electronic as well as the local structural changes would appear in the x-ray absorption near edge structure (XANES), in contrast to information of only the local structure available from EXAFS spectrum.

In this paper, we have studied high-magnetic-field Mn K-edge XANES of near half-doped manganite $Pr_{0.6}Ca_{0.4}MnO_3$. $Pr_{1-x}Ca_xMnO_3$ is known to have the charge- and orbital-ordering (COO) state in broad Ca composition $0.3 < x < 0.75$ [22]. Based on the temperature-field (T–H) phase diagram in [8], $Pr_{0.6}Ca_{0.4}MnO_3$ undergoes the COO transition at $T_{COO} \approx 235$ K at zero field. As temperature is decreased, antiferromagnetic (AFM) spin ordering and canted AFM ordering take place at $T_N \approx 170$ K and $T_{CA} \approx 40$ K, respectively. With application of magnetic field, the insulator state below T_{COO} can be transformed into the FM metal state accompanied by collapse of the COO state [8]. We have investigated the change in the electronic structure of $Pr_{0.6}Ca_{0.4}MnO_3$ by comparing the spectrum line shape of the Mn K-edge XANES at various magnetic fields. The magnetic-field dependence of XANES has been less studied than the temperature dependence in manganites. In this work, we found that the XANES slightly enhances in the COO insulator to FM metal transition and its field variation shows clear hysteresis, as seen in the metamagnetic transition. To the best of our knowledge such a distinct correlation between the XANES and the COO–FM transition has never been reported previously in any manganites. The enhancement of the Mn K-edge absorption suggests an increase in the density of states of 4p electrons of Mn ions, resulting from the reduction of the 4p–3d hybridization of the neighboring Mn ions.

2. Experimental procedure

A single crystal of $Pr_{0.6}Ca_{0.4}MnO_3$ was grown by the floating-zone method, as described in [8]. The crystal was pulverized and diluted by epoxy resin to obtain the appropriate absorption jump ($\mu t = 0.5$–1, where μ is the absorption coefficient of the x-ray and t is the sample thickness) at the Mn K-edge. The Mn K-edge XANES measurements were performed on the NW2A beamline [23] of the Photon Factory Advanced Ring, Tsukuba, Japan. A direct transmission method using a wavelength-dispersive spectrometer (the so-called DXAFS spectrometer) was used [24]. Reproducibility of the measurement is much improved by using a DXAFS spectrometer because no mechanical operation is needed. A miniature pulsed magnet

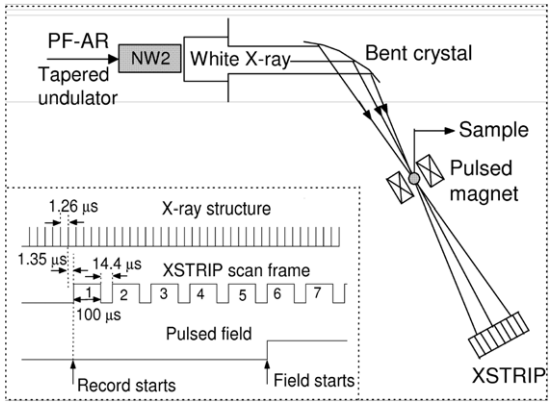

Figure 1. Schematic setup for the XANES installed at the NW2A beamline of PF-AR. Left and bottom shows the relationship among the x-ray structure, the XSTRIP frame, and the pulsed field. The pulsed field was applied from frame 6.

was used for the generation of magnetic fields [25, 26]. A silicon microstrip-based x-ray detector (XSTRIP) [27] composed of a series of frames was used so that the spectrum in each frame could be recorded in parallel in time-dependent magnetic fields.

Figure 1 shows a schematic diagram of the experimental setup, where the miniature pulsed magnet was installed into the spectrometer. The left and bottom of figure 1 shows the time chart of the x-ray pulses, the XSTRIP scan-frames and the pulsed magnetic field, as well as the related parameters. The recording was started by a trigger pulse created by one of the x-ray pulse. The number of x-ray pulses included in the Nth ($N = 1, 2, \ldots$) scan-frame (100 μs width) was kept constant during the following measurements. The pulsed magnetic field had a duration time of ~1 ms and a maximum of 12 T at 0.4 ms, as shown later in figure 4(a). The pulse was tuned so that the field started at frame 6, reached a maximum at the center of frame 9 ($114.4 \times 3.5 = 0.4$ ms), and reduced to zero at frame 14. Thus, the change in the field in frame 9 was smaller (~0.2 T) than in the other frames, which was important for a stable XANES experiment. The final XANES spectrum was obtained by the statistical average after approximately 50 magnetic-field pulses. The combination of a DXAFS spectrometer, a pulsed magnetic field and a fast detector XSTRIP enables us to make very accurate measurement without any thermal or mechanical fluctuation in timescales longer than 1 ms which is the duration of the pulsed field. This sort of field-modulation technique allows us to detect a tiny change of spectrum by magnetic field.

The magnetization measurements were also performed to investigate the critical field of the insulator to metal transition because a critical field for the field-induced transition would be dependent on the field sweep rate.

3. Results and discussion

The magnetization (M) curve measured in a pulsed magnetic field (H) exhibits clear metamagnetic transition in both H-increasing and H-decreasing processes, as can be seen from

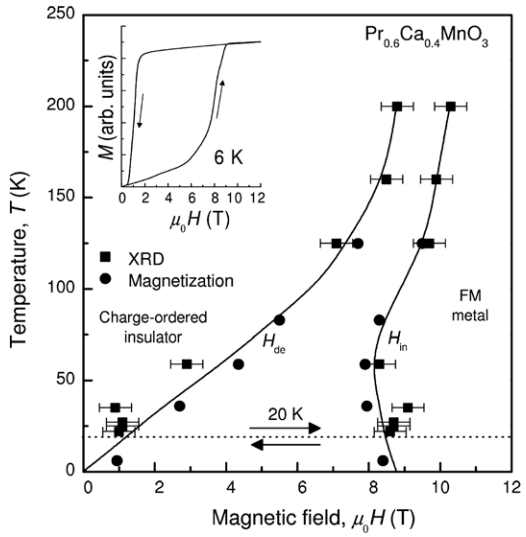

Figure 2. Temperature-and magnetic-field phase diagram of $Pr_{0.6}Ca_{0.4}MnO_3$ deduced by XRD (the intensity for (220) reflection) [25] and magnetization measurements in pulsed magnetic fields. The solid lines are guides to the eyes. The area between the lines shows the magnetic hysteresis region.

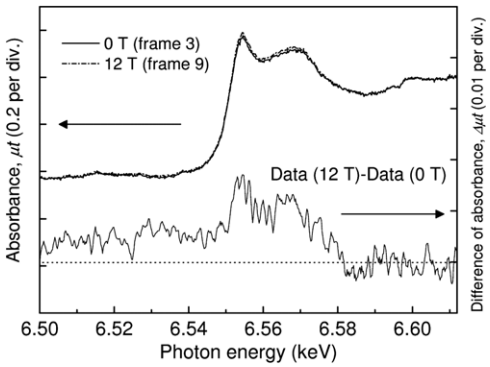

Figure 3. Bottom and left axes: the 20 K XANES measured at zero field (frame 3) and 12 T (frame 9). Bottom and right axes: difference between zero-field data and 12 T data.

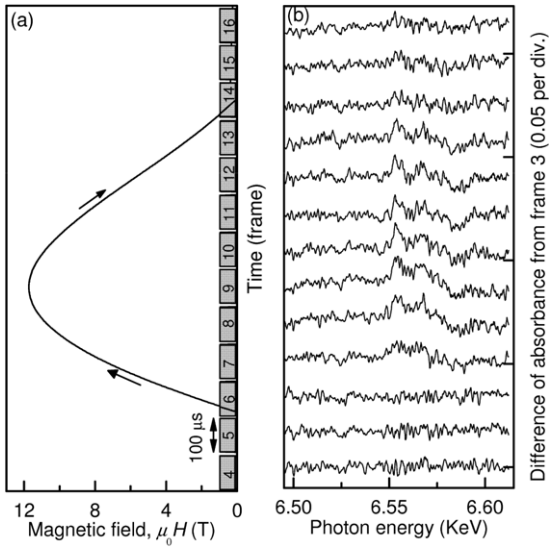

Figure 4. (a) The pulsed magnetic field consists of a series of frames, each having duration of 100 μs. In each pulse, the field starts increasing at frame 6, reaches a maximum at frame 9 and reduces to zero at frame 14. (b) Differences between zero-field XANES (frame 3) and those recorded at different fields (frames 4–16) at 20 K.

the 6 K data shown in the inset of figure 2. The critical field for the transition is deduced by the peak position of dM/dH. Figure 2 shows that the critical field for the COO insulator to FM metal transition in the H-increasing process (H_{in}) is slightly larger than that reported earlier [8], which is clear at low temperatures, whereas the critical field for the metal–insulator transition in the H-decreasing process (H_{de}) exhibits an inverse variation. In figure 2, we also plot the critical fields obtained by the previous x-ray diffraction (XRD) experiment in pulsed magnetic fields [25]. The hysteresis region between H_{in} and H_{de} is larger than that of the magnetization data. This is easy to understand recalling that in the magnetization measurement, the typical field sweep rate at H_{in} was 5 T ms^{-1}, while it was 100 T ms^{-1} for the XRD measurement. In the present work, the pulsed field has a sweep rate of ~30 T ms^{-1} at H_{in} and an intermediate critical field is expected, as shown by the guides to the eyes in figure 2. At 20 K, $\mu_0 H_{in}$ and $\mu_0 H_{de}$ are estimated to be 8.5 T and 1.0 T, respectively.

Figure 3 shows the 20 K XANES spectra of $Pr_{0.6}Ca_{0.4}MnO_3$ at zero field (frame 3) and 12 T (frame 9), the maximum of the pulsed field. The sharp main edge peak is found at 6.554 keV and another peak is at an energy position higher by about 14 eV. This two-peak structure is common in manganites and reflects the broad density of state (DOS) of Mn 4p [21]. Since the spectrum measured using the dispersive method is sensitive to the homogeneity of the sample and our powder sample has some inhomogeneity, the fine structures such as the preedge peak [4] expected at the lower energy region of the main edge are smeared out in the present work. When a field of 12 T, which is much larger than the critical field ($\mu_0 H_{in} = 8.5$ T) required to induce the insulator to metal transition, was applied, the shape of the spectrum is still quite similar to that at zero field. A close scrutiny reveals that the two peaks in the spectrum are slightly enhanced at 12 T compared to that at zero field. Although the difference is quite small, as shown in figure 3, our measurement system can detect this small change with high stability. On the other hand, we found no clear shift of the peaks by applying magnetic fields.

Figure 4 shows the difference of the absorption spectrum between zero-field data (frame 3) and those recorded at different fields (frames 4–16). No difference of absorption is detected from frames 4 to 6 where the magnetic field is zero or lower than the critical field $\mu_0 H_{in} \approx 8.5$ T. From frame 7, the field at the frame center approaches H_{in} and a significant difference of the spectrum is observed. With increasing the field, the intensity of the differential spectrum is enhanced and reaches a maximum at 12 T (frame 9). While the field is removed, the differential spectrum is gradually reduced and nearly disappears below the other critical field $\mu_0 H_{de} \approx 1$ T (frame 14). We note that, although the magnetic field varies by 0.2–4 T within a scan-frame, the central-frame-field dependence of the integrated intensity of

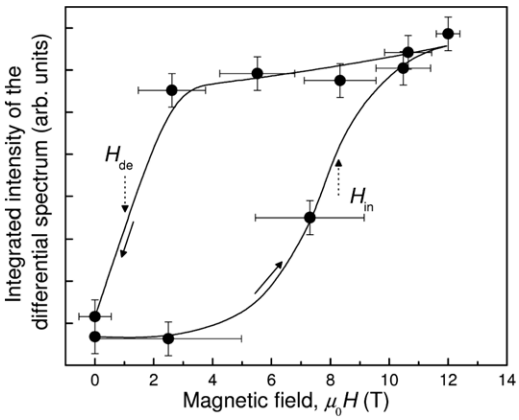

Figure 5. Magnetic-field dependence of the integrated intensity of the differential spectrum around the Mn main edge (6.540–6.584 keV). The solid curves are guides to the eyes. The solid arrows show the directions of the field change. The dotted arrows denote the critical fields H_{in} and H_{de} deduced from figure 2.

the differential spectrum shown in figure 5 presents a clear hysteresis, indicating that in both the H-increasing and H-decreasing processes, the XANES data are in agreement with the results of the XRD and magnetization experiments (see figure 2). Thus, a reversible insulator–metal transition accompanied by a large hysteresis is observed by the evolution of the differential XANES spectrum with magnetic field.

A recent report on $LaMnO_3$ revealed that in the lattice-distorted PM state, an application of pressure can slightly enlarge the XANES spectrum, which is correlated with a total removal of the local Jahn–Teller distortion of the Mn sites [7]. This suggests that in $Pr_{0.6}Ca_{0.4}MnO_3$, the enhancement of XANES spectrum is also related to local distortion. However, theoretical simulation of XANES in $LaMnO_3$ at high pressures only produces the enhancement of the main edge peak [7], different from the experimental results where both the main edge and the next peaks are clearly enhanced. Hence, other effects (e.g. the hybridization effect) beyond the localized pictures are required for understanding the change in XANES when the Jahn–Teller distortion is removed.

As the hybridization between the 4p state of the central Mn ion with the core hole and the 3d state of neighboring Mn ions is significant [21] because of the large spatial extent of the 4p wavefunction, it is not unreasonable to expect a change in the 4p–3d hybridization strength by removal of the local distortion. The enhancement of XANES suggests the increase of the 4p DOS, hence, the decrease of the 4p–3d hybridization. Since the hybridization of Mn 3d with O 2p is expected to enlarge in magnetic fields by reduction of the distortion and tilting of the MnO_6 octahedron, the decrease of the 4p–3d hybridization in magnetic fields indicates that the 4p–3d hybridization of neighboring Mn ions is caused by a direct overlap of the wavefunctions not by the interaction through the O 2p orbital.

It is worth noting that in the CMR compounds $La_{1-x}Ca_xMnO_3$ ($\sim 0.2 < x < 0.5$), a dip-peak structure with 2 eV splitting in the differential spectrum was observed below T_C [4]. Such a peculiar feature suggests that compared to the edge structure at low temperatures (FM phase) the edge

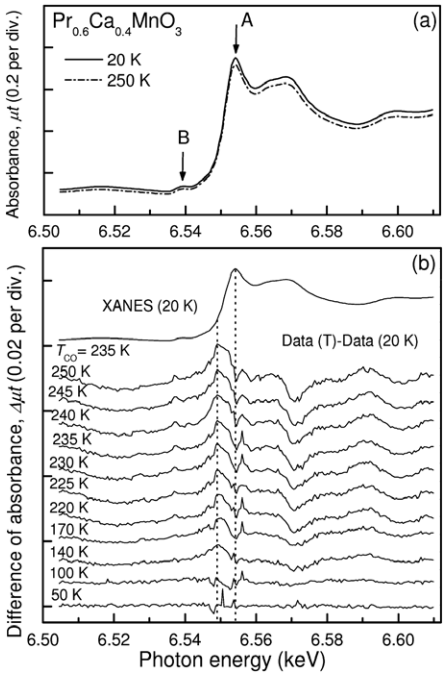

Figure 6. (a) Zero-field XANES measured at 20 and 250 K. (b) Temperature dependence of the differential spectrum calculated by subtracting the 20 K data.

above T_C (PM phase) is actually broadened [4]. For the COO compounds ($x > 0.5$), a dip-peak structure similar to that observed in the CMR samples was also observed in the differential spectrum below T_N but the phase is inverted [4]. The local distortion in the COO phase is enhanced compared to the PM phase; the distortion in the latter being larger than that in the FM phase. Thus, like the low-temperature high-field phase (FM metal), the XANES in the zero-field high-temperature phase (PM) should be enhanced compared to the zero-field low-temperature phase (COO AFM). To clarify this point, we finally examined the evolution of XANES through the charge- and orbital-ordering transition at $T_{COO} \approx 235$ K by a conventional step-scan method at zero field. The result shows that all the XANES spectra exhibit similar shape and no significant shift of either the main edge structure (A) or the preedge structure (B) is detected, as can be seen from the 20 K and 250 K data (figure 6(a)). Thus, the local electronic structure of the Mn ion is essentially the same above and below the charge-ordering transition temperature. In fact, we tried to obtain a hysteresis loop similar to figure 5 from XANES at different temperatures. However, it is difficult to determine whether the XANES above T_{COO} is enhanced or not because a slight movement of the sample caused by the thermal contraction of the cooling devices leads to a small change in the absorption depending on the position of the sample (see figure 6(a)). To avoid the thermal effect, the main edge peaks of all the XANES data are normalized and a differential spectrum was evaluated by subtracting the data at 20 K, as shown in figure 6(b). The resulting temperature-induced difference of the spectrum exhibits a quite similar shape to that deduced in the field-induced insulator–metal transition (figures 3 and 4). Note that the normalized data shown in figure 6(b) are only

an approximation. There is no such a problem for the data of figures 3 and 4, where the temperature is stable.

A comparison between both the differential spectra reveals that: (i) compared to the field-induced differential spectrum the temperature-induced one presents a 5 eV-shift towards the lower energy, the reason for which might be due to the change of the lattice constants with temperature; (ii) the field-induced differential spectrum is enhanced only when the magnetic field exceeds the critical field H_{in}, while the temperature-induced differential spectrum grows gradually with increasing temperature. The latter originates from two aspects of contributions. One is that the structural change at T_{COO} in $Pr_{0.6}Ca_{0.4}MnO_3$ can be a broad transition as was observed in $Pr_{0.5}Ca_{0.5}MnO_3$ [9, 28]. The other is that the change of the distortion through T_{COO} itself might be small in magnitude, as discussed above, and be difficult to detect experimentally.

4. Conclusions

We have reported the magnetic field and temperature dependencies of the Mn K-edge XANES spectrum of nearly half-doped manganite, $Pr_{0.6}Ca_{0.4}MnO_3$, with the focus mainly on the field dependence. The XANES spectrum is slightly enhanced when the field exceeds the critical field required for the COO insulator to FM metal transition. We found that the magnetic-field dependence of the XANES enhancement shows a large hysteresis effect, corresponding to the metamagnetic transition observed by magnetization measurements. Such a clear correlation of the K-edge XANES and magnetism has been observed for the first time in manganites. Since the DOS of 4p electrons in Mn should be affected by the COO–FM transition that is closely related to the change in the local distortion, the observed enhancement of XANES is due to the change in the Mn 4p DOS. A slight reduction of the hybridization between the 4p state of the central Mn ion with the core hole and the 3d state of the neighboring Mn ions can explain the enhancement of the 4p DOS. The obtained magnetic-field variation of XANES is useful for clarifying the interplay between the 4p and 3d electrons of Mn ions; it is crucial for a better understanding of the resonant x-ray scattering using the Mn K-edge transition. For quantitative discussion, however, a theoretical simulation of the XANES spectrum at high magnetic field is required.

Acknowledgments

We acknowledge Professors S Kishimoto and T Sasaki for technical support and useful suggestions. We thank Professor Iwasawa for installing the high-speed position sensitive detector XSTRIP to the NW2A and permitting us to use it. YHM thanks Professors Y Murakami, H Sawa, M Nomura, and H Kawata for valuable discussions. This work is partly supported by PRESTO of the Japan Science and Technology Agency and by a Grant-in-Aid for Scientific Research on Priority Areas 'High Field Spin Science in 100 T' (No. 451) from the Ministry of Education, Culture, Sports, Science, and Technology (MEXT), and by the Japan Society for the Promotion of Science. Synchrotron radiation experiments were carried out under the Photon Factory Experimental Program No. 2007G073.

References

[1] Jin S, Tiefel T H, McCormack M, Fastnacht R A, Ramesh R and Chen L H 1994 *Science* **264** 413
[2] Schiffer P, Ramirez A P, Bao W and Cheong S W 1995 *Phys. Rev. Lett.* **75** 3336
[3] Subías G, García J, Proietti M G and Blasco J 1997 *Phys. Rev.* B **56** 8183
[4] Bridges F, Booth C H, Anderson M, Kwei G H, Neumeier J J, Snyder J, Mitchell J, Gardner J S and Brosha E 2001 *Phys. Rev.* B **63** 214405
[5] Qian Q, Tyson T A, Kao C-C, Croft M, Cheong S-W, Popov G and Greenblatt M 2001 *Phys. Rev.* B **64** 024430
[6] Sánchez M C, Subías G, García J and Blasco J 2003 *Phys. Rev. Lett.* **90** 045503
[7] Ramos A Y, Tolentino H C N, Souza-Neto N M, Itié J P, Morales L and Caneiro A 2007 *Phys. Rev.* B **75** 052103
[8] Tomioka Y, Asamitsu A, Kuwahara H, Moritomo Y and Tokura Y 1996 *Phys. Rev.* B **53** R1689
[9] Zimmermann M v, Hill J P, Gibbs D, Blume M, Casa D, Keimer B, Murakami Y, Tomioka Y and Tokura Y 1999 *Phys. Rev. Lett.* **83** 4872
[10] Zener C 1951 *Phys. Rev.* **82** 403
[11] Okimoto Y, Katsufuji T, Ishikawa T, Urushibara A, Arima T and Tokura Y 1995 *Phys. Rev. Lett.* **75** 109
[12] Millis A J, Littlewood P B and Shraiman B I 1995 *Phys. Rev. Lett.* **74** 5144
[13] Millis A J, Shraiman B I and Mueller R 1996 *Phys. Rev. Lett.* **77** 175
[14] Röder H, Zang J and Bishop A R 1996 *Phys. Rev. Lett.* **76** 1356
[15] Tyson T A, Mustre de Leon J, Conradson S D, Bishop A R, Neumeier J J, Röder H and Zang J 1996 *Phys. Rev.* B **53** 13985
[16] Booth C H, Bridges F, Kwei G H, Lawrence J M, Cornelius A L and Neumeier J J 1998 *Phys. Rev. Lett.* **80** 853
[17] Booth C H, Bridges F, Kwei G H, Lawrence J M, Cornelius A L and Neumeier J J 1998 *Phys. Rev.* B **57** 10440
[18] Hwang H Y, Cheong S-W, Radaelli P G, Marezio M and Batlogg B 1995 *Phys. Rev. Lett.* **75** 914
[19] Bindu R, Pandey S K, Kumar A, Khalid S and Pimpale A V 2005 *J. Phys.: Condens. Matter* **17** 6393
[20] Stöhr J 1992 *NEXAFS Spectroscopy* (Berlin: Springer)
[21] Elfimov I S, Anisimov V I and Sawatzky G A 1999 *Phys. Rev. Lett.* **82** 4264
[22] Jirak Z, Krupicka S, Simsa Z, Dlouha M and Vratislav S 1985 *J. Magn. Magn. Mater.* **53** 153
[23] Mori T, Nomura M, Sato M, Adachi H, Uchida Y, Toyoshita A, Yamamoto S, Tsuchiya K, Sioya T and Kawata H 2003 *AIP Conf. Proc.* **705** 255
[24] Inada Y, Suzuki A, Niwa Y and Nomura M 2006 *AIP Conf. Proc.* **879** 1230
[25] Matsuda Y H, Ueda Y, Nojiri H, Takahashi T, Inami T, Ohwada K, Murakami Y and Arima T 2004 *Physica* B **346/347** 519
[26] Matsuda Y H, Inami T, Ohwada K, Murata Y, Nojiri H, Murakami Y, Ohta H, Zhang W and Yoshimura K 2007 *J. Phys. Soc. Japan* **76** 034702
[27] Salvini G, Headspith J, Thomas S L, Derbyshire G, Dent A, Rayment T, Evans J, Farrow R, Diaz-Moreno S and Ponchut C 2005 *Nucl. Instrum. Methods* **551** 27
[28] Jirák Z, Damay F, Hervieu M, Martin C, Raveau B, André G and Bourée F 2000 *Phys. Rev.* B **61** 1181